Magnetic Reconnection in the Solar Atmosphere
ASP Conference Series, Vol. 111, 1996
R.D. Bentley and J.T. Mariska, (eds.)

Energetic Consequences of the DC-Electric Field Model

NASA-CR-204581

Dominic M. Zarro

Applied Research Corporation, NASA/GSFC Code 682.3, Greenbelt, MD 20771, USA

Richard A. Schwartz

Hughes/STX, NASA/GSFC Code 682.3, Greenbelt, MD 20771, USA

Abstract. We analyze a solar flare observed simultaneously in soft and hard X-rays by instruments onboard *Yohkoh* and the *Compton Gamma Ray Observatory*. Assuming a simple one-dimensional coronal loop that is heated by field-aligned currents, we solve the energy balance equation to derive the DC-electric field strength necessary to explain the observed soft X-ray emission by current-dissipation. We use the derived DC-electric field to predict the number flux of electrons accelerated by thermal runaway and compare this prediction with the number flux of nonthermal thick-target electrons implied by impulsive phase hard X-ray observations. We find that runaway acceleration can account for the large flux ($\gtrsim 10^{36}$ s^{-1}) of nonthermal electrons provided the loop filling factor is $\lesssim 10^{-3}$ such that heating and acceleration occur in filamented structures within the loop.

1. Introduction

Magnetic field line reconnection models predict DC-electric field components parallel to the loop magnetic field (Tsuneta 1995). It has been proposed that such DC-electric fields can produce nonthermal electrons in solar flares via thermal runaway acceleration (Tsuneta 1985, Holman 1985). In particular, a DC-electric field will accelerate thermal electrons until a steady state current is established. Since the collisional drag on the electrons decreases with increasing velocity, those electrons with velocities above a critical velocity will undergo runaway acceleration producing nonthermal electrons that emit hard X-ray radiation via thick-target interactions (Holman, Kundu, and Kane 1989). Electrons below the runaway threshold continue to heat the loop plasma producing soft X-ray emission. This paper investigates the energetics of the DC-electric field model by examining whether the DC-electric field strength implied by soft X-ray heating is sufficient to account for the number flux of nonthermal electrons implied by hard X-ray observations.

In the following section, we derive the DC-electric field strength by solving the energy balance equation in a single loop with uniform cross-sectional area. As input to this equation, we use simultaneous soft and hard X-ray observations from *Yohkoh* and the *Compton Gamma Ray Observatory (CGRO)* of a

simple loop flare that occurred on 1992 September 6. From the *Yohkoh* Soft X-ray Telescope (SXT), we infer the geometry of the flaring loop. From the *Yohkoh* Bragg Crystal Spectrometer (BCS), we derive the temperature T and emission measure EM of the flare source. From the *CGRO* Burst and Transient Spectrometer Experiment (BATSE), we deduce the number flux of accelerated electrons.

2. Method

For a one-dimensional loop, the energy balance equation is expressed as

$$\frac{dU}{dt} = Q - R - \frac{dF_c}{dz} - 5nkT\frac{dv}{dz}, \tag{1}$$

where $U = 3nkT$ is the thermal energy per unit volume, Q is the total flare heating rate, $F_c \simeq -10^{-6}T^{5/2}dT/dz$ is the Spitzer conductive heat flux, $R \simeq an^2T^{-1/2}$ is the optically thin cooling rate, and the velocity gradient term is the enthalpy flux of convective motions within the loop. For the radiative cooling coefficient, we use $a = 2.2 \times 10^{-19}$ which is based on calculations by Raymond, Cox, and Smith (1976). We shall assume that the density n and temperature T are uniform along the loop length. This assumption is valid about 20–30 s after heating onset when thermal conduction will have redistributed the heat energy throughout the loop, and hydrodynamic motions will have restored approximate pressure balance within the loop (Fisher and Hawley 1990).

We simplify equation (1) by spatially averaging it with respect to the total loop volume such that

$$\dot{U}V = QV_c - RV + [5nkTv(0) + F_c(0)]A, \tag{2}$$

where V is the total volume of the loop and V_c is the volume of the current-heated region. The enthalpy and conductive fluxes vanish at the loop apex and are negligible in the chromosphere ($z = 0$) relative to the heating and radiative cooling terms. Note that the volume of the current-heated region is assumed to be less than the total observed loop volume $V = 2AL$, where A is the observed loop area and L is the loop half-length. From the ratio of these two volumes, we define a filling factor $f = V_c/V$. Following Holman (1985), we assume that the heat energy generated within each current channel is distributed into the larger loop volume by conductive (or convective) transport processes on a timescale less than the heating timescale.

For a loop that is heated uniformly by current-dissipation, the Joule heating rate is given by

$$Q_{curr} = nkT\nu_e(E/E_D)^2 \qquad \text{ergs cm}^{-3}\text{ s}^{-1}, \tag{3}$$

where $\nu_e \approx 3.2 \times 10^2 nT^{-3/2}$ s^{-1} is the thermal collision frequency (for classical resistivity), E is the electric field strength (assumed uniform along the loop length), and $E_D = 7 \times 10^{-8}nT^{-1}$ volts cm^{-1} is the Dreicer field. The Dreicer field is the field strength at which all the electrons in the plasma undergo thermal runaway. Substituting Q_{curr} into equation (2), we derive the following analytic expression for E

$$E = E_D \sqrt{\frac{(\dot{U} + R)}{fnkT\nu_e}} \qquad (4)$$

Given n and T, we solve equation (4) for the variation of E during the flare for different values of the filling factor. Given E, we can subsequently compute the rate of runaway electrons assuming that runaway acceleration occurs within the same current-heated channels. The runaway rate is given by the formula

$$\dot{N}_{run} \simeq .35n\nu_e(E_D/E)^{3/8}\exp[-2^{1/2}(E_D/E)^{1/2} - (1/4)(E_D/E)]V_c \qquad s^{-1}, \quad (5)$$

which includes electrons that are accelerated out of the thermal distribution as well as electrons that are scattered into the runaway regime by collisions (Kruskal and Bernstein 1964). The runaway electrons that propagate along the loop will heat the plasma by Coulomb collisions, producing thick-target hard X-ray emission as they impact the chromosphere. Assuming a power-law electron energy spectrum with spectral index δ above a low-energy cutoff E_c, the total number flux of hard X-ray-producing electrons is given by

$$\dot{N}_{thick} \simeq 3 \times 10^{33}a_1(\gamma - 1)^2 B(\gamma - 1/2, 1/2)E_c^{-\gamma} \qquad s^{-1}, \qquad (6)$$

where $B(x,y)$ is the beta function, $\gamma = \delta - 1$ is the power-law spectral index, and a_1 is the power-law amplitude, respectively, of the emitted hard X-ray spectrum (Lin and Hudson 1976). The low-energy cutoff is determined by the critical energy above which thermal electrons exceed the frictional force and undergo thermal runaway. The critical energy is given by $E_{crit} = m_e(E_D/E)\nu_e^2/2$, where ν_e is the electron thermal velocity (Holman 1985).

3. Results

We apply equation (4) to an M3.3 flare that was observed by *Yohkoh* and *CGRO* at 09:00 on 1992 September 6 (Zarro, Mariska, and Dennis 1995). From least-squares fits of synthetic spectra to the BCS Ca XIX (λ 3.177 Å) resonance line, we obtain the variations of T and EM. From preflare SXT images, we infer a loop half-length $L \simeq 3 \times 10^9$ cm, a loop cross-sectional area $A \simeq 3 \times 10^{17}$ cm^2, and a total observed volume $V \simeq 2 \times 10^{27}$ cm^3. From the emission measure and filling factor, we derive the loop density $n \simeq (EM/fV)^{1/2}$. Substituting into equation (4), we compute E for different values of f.

Figure 1 shows the time variation of E for $f = 0.1$, 0.01, and 0.001. The DC-electric field strength increases with decreasing filling factor. This effect occurs because the density within the current channels is inversely proportional to f. Consequently, since $\dot{U} \sim n$, a higher electric field strength is required to sustain the enhanced heating rate within the channels. Similarly, the electric field strength increases with time during the flare rise phase because the density within the current channels increases as plasma is heated and evaporated into the loop.

We use the BATSE LAD Continuous data to derive the nonthermal parameters of the flare. This data type produces hard X-ray spectra in 16 channels
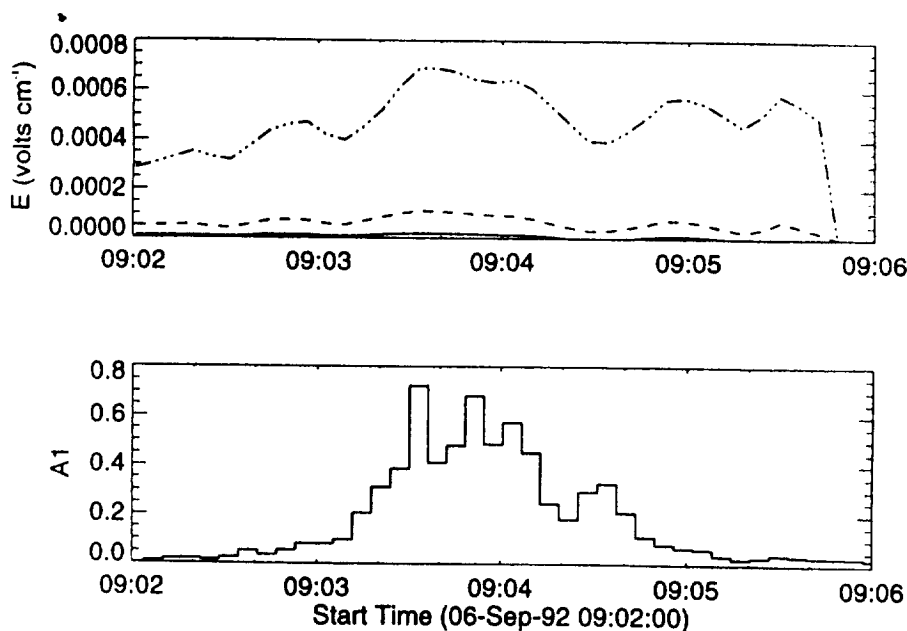
Figure 1.   Upper Panel: Variation of DC-electric field strength for filling factors $f = 0.1$ (solid), 0.01 (dash), and 0.001 (dash-dot). Lower Panel: Fitted power-law amplitude of nonthermal hard X-ray emission.

between 10 and > 1000 keV at 2.048 sec temporal resolution. The spectra show a well-defined power-law distribution of the form $I = a_1 \epsilon^{-\gamma}$ in the 20-100 keV range. From a least-squares deconvolution of the LAD response function, we obtain the temporal variations of the amplitude a_1 and spectral index γ of the power-law component. The variation of a_1 is compared with E in Figure 1. The temporal variations of these quantities are correlated such that the maximum DC-electric field coincides with the peak of hard X-ray burst emission.

For each filling factor, we use the derived values of E to compute the number flux of nonthermal electrons from the thick-target equation (6) and compare it with the number flux predicted by the runaway formula (5). Figure 2 shows this comparison for $f = 0.001$. The latter filling factor yields the optimum agreement between the measured and predicted fluxes during the rise phase of impulsive hard X-rays. For this filling factor, the peak DC-field strength is 5×10^{-4} volts cm^{-1} giving a peak runaway flux of 3×10^{37} s^{-1}. Such a high flux is a direct consequence of the low cutoff energy ($E_c \approx 10$ keV) implied by the critical energy for thermal runaway.

For $f > 0.001$, runaway acceleration alone does not produce sufficient nonthermal electrons to match the observed flux. In this case, the density within the current-heated region is too low to provide a large enough population of thermal electrons to undergo runaway. For $f < 0.001$, runaway acceleration also fails to match the observed number flux. Examination of equation (5), shows
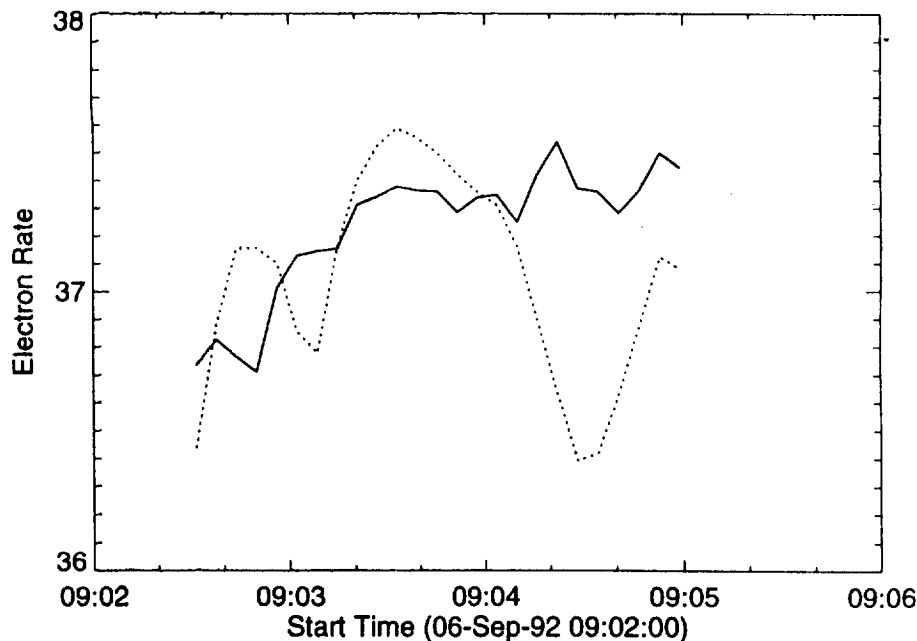
Figure 2. Comparison between the number flux of nonthermal electrons implied by hard X-ray observations (solid) and the number flux predicted by runaway acceleration for a volume filling factor of 0.001 (dashed).

that $\dot{N}_{run} \sim \exp(-E_D/E)$. Since $E_D \sim n$, the runaway rate drops exponentially with increasing density. Physically, the runaway electrons become thermalized by collisions when the density in the current-heated region becomes very large.

The predicted and observed electron fluxes show a large discrepancy after hard X-ray maximum ($\approx$ 09:04 UT) and cannot be reconciled with any value of f. This discrepancy reflects a breakdown in many of the simplifying assumptions that underly the energy-balance analysis. First, the assumption of a filling factor that is constant in time is likely to become invalid as the flare energy is distributed throughout the loop system and the heating extends to possibly multiple loops. Second, the assumption that the hard X-ray emission is predominantly nonthermal (and thick-target in origin) becomes questionable when the temperature within the heated region becomes very high and the apparent power-law spectrum is actually the result of a strong thermal bremsstrahlung component. The present soft and hard X-ray observations cannot distinguish this case.

4. Conclusions

We conclude from energy balance that DC-electric field heating and acceleration can self-consistently explain thermal soft X-ray emission and nonthermal

n acceleration in solar flares provided that heating and acceleration occur .mented subregions with a coronal loop. The filamentation is necessary to insure a sufficiently high density of thermal electrons to undergo runaway acceleration. Such filamentation of loop plasma is in fact necessitated by electrodynamic arguments. In particular, for a loop current system to remain stable, the induction magnetic field of the current-carrying electrons (including accelerated electrons) within each channel must be less than the ambient magnetic field strength. For a cylindrical geometry, this constraint enforces the following upper limit on the volume of the acceleration region (Holman 1985)

$$V_j \lesssim \frac{LB^2}{4\pi n^2 e^2}\left(\frac{c}{v_e}\right)^2\left(\frac{E_D}{E}\right)^2,\tag{7}$$

where B is the loop magnetic field strength. To satisfy this constraint, the acceleration region must be fragmented into $n_c = V_c/V_j$ multiple filaments. Adopting a typical loop field strength of $B = 100$ Gauss, and using the value of E computed at hard X-ray maximum for $f = 0.001$, we deduce a peak $n_c \simeq 10^{12}$. The existence of such a large number of current filaments introduces serious problems for maintaining charge-neutrality in the loop plasma. One possible solution is that the current systems are closed by cross-field drifting of protons at the chromospheric footpoints (Emslie and Henoux 1995).

References

Fisher, G., & Hawley, S. 1990, ApJ, 357, 243

Holman, G. 1985, ApJ, 293, 584

Holman, G., Kundu, M., & Kane, S. 1989, ApJ, 345, 1050

Emslie, A. G., & Henoux, J.-C. 1995, ApJ, 446, 371

Kruskal, M., & Bernstein, I. 1964, Phys. Fluids, 7, 407

Lin, R., & Hudson, H. 1976, Solar Phys. 50, 153

Raymond, J.C., Cox, D.P., & Smith, B.W. 1976, ApJ, 204, 290

Tsuneta, S. 1985, ApJ, 290, 353

Tsuneta, S. 1995, PASJ, 47, 691

Zarro, D., Mariska, J., & Dennis, B. 1995, ApJ, 440, 888